Antiferromagnetic Order in Epitaxial FeSe Films on $SrTiO_3$

Y. Zhou,[1] L. Miao,[2] P. Wang,[1] F. F. Zhu,[2] W. X. Jiang,[2] S. W. Jiang,[1] Y. Zhang,[1] B. Lei,[3,4,5] X. H. Chen,[3,4,5] H. F. Ding,[1,5] Hao Zheng,[2,5] W. T. Zhang,[2,5] Jin-feng Jia,[2,5] Dong Qian,[2,5,*] and D. Wu[1,5,†]

[1]*National Laboratory of Solid State Microstructures and Department of Physics, Nanjing University, Nanjing 210093, China*
[2]*Key Laboratory of Artificial Structures and Quantum Control (Ministry of Education), School of Physics and Astronomy, Shanghai Jiao Tong University, Shanghai 200240, China*
[3]*Hefei National Laboratory for Physical Sciences at Microscale and Department of Physics, University of Science and Technology of China and Key Laboratory of Strongly-Coupled Quantum Matter Physics, Chinese Academy of Sciences, Hefei, Anhui 230026, China*
[4]*High Magnetic Field Laboratory, Chinese Academy of Sciences, Hefei, Anhui 230031, China*
[5]*Collaborative Innovation Center of Advanced Microstructures, Nanjing 210093, China*

(Received 15 September 2017; published 27 February 2018)

Single monolayer FeSe film grown on a Nb-doped $SrTiO_3(001)$ substrate shows the highest superconducting transition temperature ($T_C \sim 100$ K) among the iron-based superconductors (iron pnictides), while the T_C value of bulk FeSe is only ~8 K. Although bulk FeSe does not show antiferromagnetic order, calculations suggest that the parent FeSe/$SrTiO_3$ films are antiferromagnetic. Experimentally, because of a lack of a direct probe, the magnetic state of FeSe/$SrTiO_3$ films remains mysterious. Here, we report direct evidence of antiferromagnetic order in the parent FeSe/$SrTiO_3$ films by the magnetic exchange bias effect measurements. The magnetic blocking temperature is ~140 K for a single monolayer film. The antiferromagnetic order disappears after electron doping.

DOI: 10.1103/PhysRevLett.120.097001

The pairing mechanism of high-temperature superconductors including cuprates and iron pnictides is one of the biggest challenges in modern physics. The antiferromagnetic (AFM) interaction has been long thought to correlate with high-temperature superconductivity [1,2] because the superconducting state usually appears after the AFM order is suppressed [3,4]. The AFM spin fluctuations were proposed to play an important role in the pairing of iron pnictides [1,3,5]. Among various iron pnictides, FeSe has the simplest crystalline structure [6]. The T_C value of bulk FeSe is ~8 K and can increase to ~37 K under high pressure [7]. Unlike other iron pnictides, bulk FeSe crystals do not show AFM order [7] unless a certain pressure is applied [8–10].

Surprisingly, a single monolayer (1-ML) FeSe film grown on a Nb-doped $SrTiO_3(001)$ ["STO" will refer to Nb-doped $SrTiO_3(001)$] substrate after electron doping (through the annealing process) shows a large superconducting gap (~20 meV) [11] that survives up to ~65 K [12,13]. Diamagnetic signals below ~65 K have also been reported [14]. Recently, the *in situ* resistance measurements showed that T_C value of the 1-ML FeSe/STO film can be as high as 109 K [15]. The mechanism of such a high T_C value is still an open question. Calculations have shown that the electron-phonon coupling is significantly enhanced [16] due to the interfacial effect and therefore enhances the value of T_C in this system [17], but the initial pairing mechanism is still unclear. First-principles calculations have shown that the FeSe/STO interface could enhance the AFM interaction, which helps maintain large spin fluctuations under heavy electron doping [18]. Magnetic frustration induced by the combination of the electron doping and the phonons is another possible mechanism for the superconductivity [19]. Density functional theory (DFT) calculations have suggested that the magnetic ground state of 1-ML FeSe/STO film is AFM [18,20,21]. A recent work also claimed that 1-ML FeSe/STO could be in AFM order to form topological superconductivity [22]. Therefore, it is very interesting to study the magnetic ground state of the 1-ML film before electron doping. Experimentally, the magnetic state of the FeSe/STO films is barely known. Previous angle-resolved photoemission spectroscopy (ARPES) measurements showed indirect signatures of the spin density wave [12], but they are indistinguishable from electronic nematicity [23–25]. To determine the magnetic state, regular techniques such as neutron scattering, muon spin rotation, and the Mössbauer effect have limited sensitivity for ultrathin films. In this Letter, we present direct evidence indicating that the magnetic ground state of the parent 1-ML FeSe/STO film is AFM by using magnetic exchange bias effect (MEBE) [26] measurements.

FeSe/STO films were grown following previous reports [9,15]. Films before postannealing are called "as-grown" films. The as-grown films were postannealed at ~500 °C for 4–8 h *in situ* to make them superconducting. Before the films were transferred to another chamber to grow an $Fe_{21}Ni_{79}$ layer, a 50-nm-thick Se protecting layer was grown. The polycrystalline $Fe_{21}Ni_{79}$ film was grown on

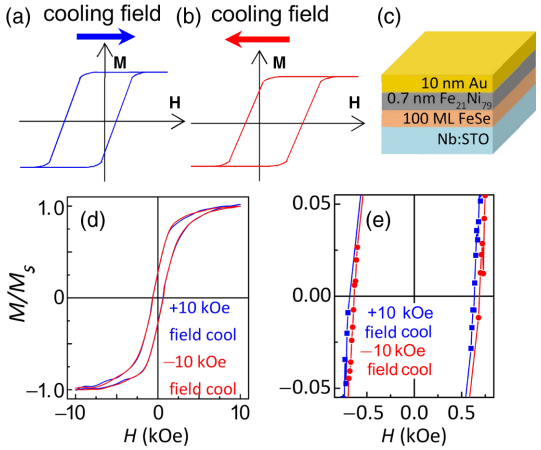

FIG. 1. The MEBE in an $Fe_{21}Ni_{79}$/FeSe/STO film. (a), (b) The schematic MHLs of the MEBE after the positive and negative FC. (c) Layout of the film. (d) MHLs of the sample in (c) measured at 5 K after FC from room temperature to 5 K. (e) The corresponding enlarged plots near the zero field.

the FeSe film at room temperature by *e*-beam evaporation after removing the Se protecting layer by properly annealing at 400 °C. The $Fe_{21}Ni_{79}$ thickness was optimized for MEBE measurements. Finally, a 10 nm Au film was deposited to prevent oxidation. ARPES were performed at ARPES Beamline of National Synchrotron Radiation Laboratory in Hefei and at Beamline 4.0.3 of Advanced Light Source. Magnetic properties were measured by a Quantum Design SQUID-VSM system. The magnetic field (**H**) was set to zero in an oscillation mode to reduce the residual field of the magnet before measurements. The residual field was further calibrated by a reference sample of Au/$Fe_{21}Ni_{79}$(10 nm)/STO [see the Supplemental Material (SM) [27]]. The coercivity of the magnetic hysteresis loop (MHL) is obtained by linearly fitting the data points very close to the zero magnetization points. Details on how to determine the coercivity with high accuracy and also how to determine the uncertainty is described in the SM [27].

The MEBE is widely used for probing the AFM order in materials, particularly in thin films [26,28]. The MEBE occurs in a ferromagnet-antiferromagnet heterostructure when it is cooled in an external **H** through the Néel temperature (T_N) of the AFM layer or is grown in an external field. The MEBE relies on the interfacial magnetic exchange coupling between the AFM and ferromagnetic (FM) layers. Measurements are on the magnetization (**M**) of the FM layer. The distinct phenomenon of the MEBE is that the center of the MHL shifts away from the $\mathbf{H} = 0$ point; i.e., the absolute values of the coercive fields for increasing (H_{C+}) and decreasing (H_{C-}) fields are different. More importantly, the shifting direction reverses when the cooling field (CF) is reversed, as illustrated in Figs. 1(a) and 1(b).

First, we studied the thick FeSe/STO to show the capability of MEBE measurements on an FeSe system. Polycrystalline $Fe_{21}Ni_{79}$ is used as the FM layer. Figures 1(d) and 1(e) present the MHLs and the corresponding enlarged plots of a Au(10 nm)/$Fe_{21}Ni_{79}$(0.7 nm)/FeSe(100 ML)/STO sample measured at 5 K after field cooling (FC) from room temperature. The CF is either +10 kOe or −10 kOe. The linear background originating from the diamagnetic signal of the STO substrate is subtracted from the raw data (see the SM [27]). In Fig. 1(e), the MHLs shift away from the $\mathbf{H} = 0$ point, and the shifting direction is the opposite of the direction of the CF. The shift of the MHLs and the reverse of the shifting direction upon reversing the CF indicate that the observed effect is the MEBE. From Fig. 1(e), we obtain the magnitude of the shift—the exchange bias field (H_{EB}) $= |H_{C-} - H_{C+}|/2 \sim 28 \pm 2.5$ Oe. The observed MEBE persists up to about 180 K in this sample.

Previous experiments have shown that a capping layer degrades the superconducting properties of 1-ML FeSe/STO [29]. Even an innocuous FeTe overlayer can hole dope the system [30], provide coupling to phonon modes [31], or intermix Te and Se atoms [32]. Therefore, it is necessary to examine the possibility of the observed AFM order induced by the $Fe_{21}Ni_{79}$ overlayer. First, it is impossible that the AFM order is induced by $Fe_{21}Ni_{79}$ via the interfacial magnetic interaction. Instead, a FM layer can alter a non-FM material to a FM order, known as magnetic proximity effect [33–35] (more discussion in the SM [27]). Second, other interfacial effects, such as the selenized $Fe_{21}Ni_{79}$ film, the interfacial intermixing, and the alternation of Se height from the Fe plane [36] could lead to an AFM order. It is crucial to carry out control experiments to verify that the observed MEBE is the intrinsic property of the as-grown FeSe/STO films. (i) First, we prepared a sample of Au(10 nm)/$Fe_{21}Ni_{79}$(0.7 nm)/STO [Fig. 2(a)] and conducted the same measurements. Figures 2(b) and 2(c) show

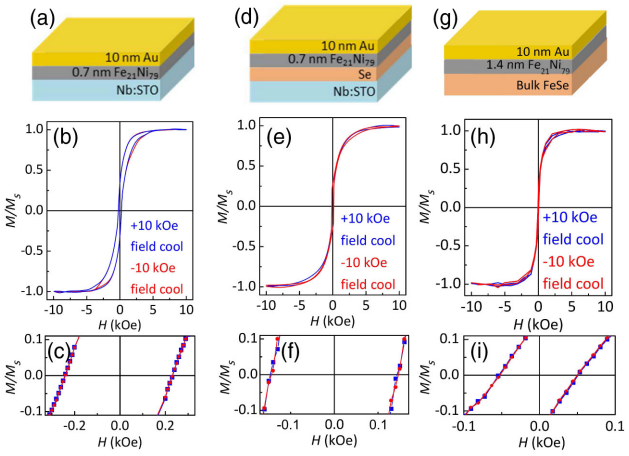

FIG. 2. Control experiments. (a) Layout of control sample 1. (b) MHLs and (c) the corresponding enlarged plots of the sample in (a). (d) Layout of control sample 2. (e) MHLs and (f) the corresponding enlarged plots of the sample in (d). (g) Layout of control sample 3. (h) MHLs and (i) the corresponding enlarged plots of the sample in (g). The loops did not shift in all of the control experiments.

the MHLs and the enlarged plots. No shift was detected within our experimental uncertainty, which excludes any technical problems. (ii) Before the deposition of the $Fe_{21}Ni_{79}$ film, the FeSe/STO film was annealed to remove the Se protecting layer. Therefore, the $Fe_{21}Ni_{79}$ film might have been selenized by the possible residual Se to form an AFM layer at the interface and lead to MEBE. To exclude this possibility, we fabricated a control sample of Au(10 nm)/$Fe_{21}Ni_{79}$(0.7 nm)/Se(50 nm)/STO [Fig. 2(d)]. Figures 2(e) and 2(f) show the MHLs and the enlarged plots. Clearly, the loops do not shift, suggesting that the selenized $Fe_{21}Ni_{79}$ film is not AFM. (iii) We also exclude the possibility that the AFM layer is caused by the intermixing, alloying, and proximity (polarization) effect between the $Fe_{21}Ni_{79}$ film and the FeSe film or the change of Se height by using bulk FeSe as a reference. We prepared a sample of Au(10 nm)/$Fe_{21}Ni_{79}$(1.4 nm)/bulk FeSe [Fig. 2(g)]. Here, a 1.4-nm-thick $Fe_{21}Ni_{79}$ film is used to obtain better a signal-to-noise ratio because the high quality cleaved surface area ($\sim 1 \times 1$ mm^2) of bulk FeSe is much smaller than that of a STO substrate ($\sim 3 \times 3$ mm^2). The measurement temperature (10 K) is kept slightly above the T_C value of bulk FeSe to avoid the strong diamagnetic signal of the superconducting bulk FeSe. The cleaved bulk FeSe crystal has a (001) surface with Se termination which is the same as the FeSe/STO film. Since both interfaces (the $Fe_{21}Ni_{79}$/FeSe interface) are identical, one would expect the presence of the MEBE in the $Fe_{21}Ni_{79}$/bulk FeSe sample if the AFM layer were induced by the interfacial intermixing, alloying, polarization, or height change of the Se atoms. However, the MEBE is not observed in this control sample, as shown in Fig. 2(i). With the three control experiments above, we conclude that the observed MEBE most likely originates from the AFM layer in the 100-ML FeSe/STO film. In addition, for completeness, we note that the MEBE can also occur between a heterostructure of a ferromagnet and a spin glass system [26,28]. The spin glass state in the FeSe/STO film is excluded by the thermal remnant magnetization measurements [see the SM [27]].

To show the temperature dependence more clearly, we used the so-called inversion method to plot the MHLs. In this method, both **M** and **H** of the original loop are multiplied by −1. In other words, we invert the MHL. The new loop is called the "inverted loop." After inversion, the H_{C-} value of the original loop reflects from the negative **H** side to the positive **H** side; therefore, we can directly show the difference between H_{C+} and H_{C-}. Figures 3(a)–3(f) show the enlarged plots with original and inverted loops near $H_{C\pm}$ of a Au(10 nm)/$Fe_{21}Ni_{79}$(0.7 nm)/FeSe(100 ML)/STO sample measured at different temperature after FC. The MEBE gradually becomes weaker with increasing temperature. The temperature dependence of H_{EB} is summarized in Fig. 3(g). The blocking temperature T_B, where H_{EB} becomes zero, is ~180 K. The value of H_{EB} depends on both the AFM and FM layers, while T_B depends mainly on the AFM layer [26].

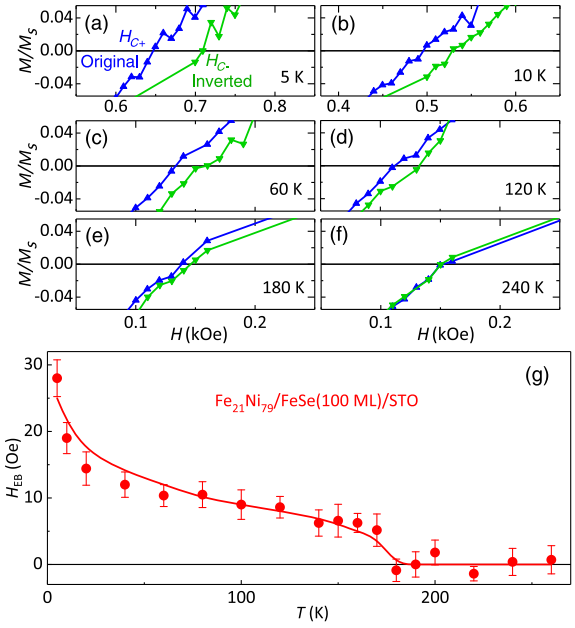

FIG. 3. Temperature dependence of the MEBE. (a)–(f) Enlarged curves of original and inverted loops of Au(10 nm)/$Fe_{21}Ni_{79}$(0.7 nm)/FeSe(100 ML)/STO film at different temperatures after FC. (g) H_{EB} as a function of temperature. The solid line is a guide for the eye.

T_B and T_N are intimately correlated and, in general, $T_N \geq T_B$ [26]. Therefore, we obtained the lower limit of T_N of ~180 K for the 100-ML FeSe/STO film. The MEBE is also carried out on the FeTe/STO film, which possesses a well-known AFM state [37,38]. The determined T_B of ~75 K is comparable to the T_N of the thick FeTe/MgO film [39] (see the SM [27]).

After the demonstration of the capability of the MEBE study on thick FeSe/STO films, we studied the 1-ML FeSe film. The as-grown 1-ML FeSe/STO film is nonsuperconducting. It becomes superconducting by doping electrons through the annealing process [11–15]. We prepared two types of samples: Au(10 nm)/$Fe_{21}Ni_{79}$(0.7 nm)/as-grown FeSe(1 ML)/STO (sample 1) and Au(10 nm)/$Fe_{21}Ni_{79}$(0.7 nm)/annealed FeSe(1 ML)/STO (sample 2). Our sample 1 is in the "*N* phase" and sample 2 the "*S* phase" as defined by He *et al.* [13]. A superconducting gap was observed on annealed FeSe/STO films by ARPES (see the SM [27]). The MEBE is clearly observed in sample 1 at 5 K after FC. Shown in Fig. 4(c), the MHLs shift away from the $\mathbf{H} = 0$, and the shifting direction reverses when the CF is reversed. The shift of the MHL is relatively small (~5 Oe), but it is still well above the error bar (~0.5 Oe). By contrast, the MEBE was not detected within our experimental uncertainty in sample 2, as shown in Fig. 4(e). Because sample 2 is heavily electron doped and no AFM order exists, we would like to propose that the heavy electron doping by the annealing process destroys the AFM order. Figures 4(f) and 4(g) show enlarged original and inverted plots near $H_{C\pm}$

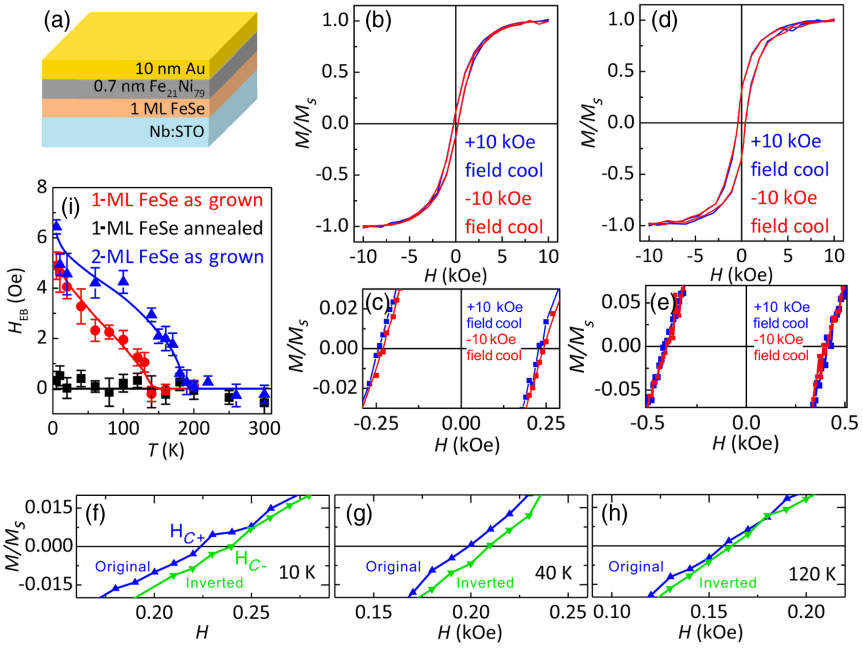

FIG. 4. The MEBE in 1-ML and 2-ML FeSe/STO films. (a) Layout of the films. (b) MHLs of Au(10 nm)/$Fe_{21}Ni_{79}$(0.7 nm)/as-grown FeSe(1 ML)/STO film and (c) the corresponding enlarged plots. (d) MHLs of Au(10 nm)/$Fe_{21}Ni_{79}$(0.7 nm)/annealed FeSe(1 ML)/STO film and (e) the corresponding enlarged plots measured at 5 K. (f)–(h) Enlarged curves of the original and inverted loops of the Au(10 nm)/$Fe_{21}Ni_{79}$(0.7 nm)/as-grown FeSe(1 ML)/STO film at three temperatures. (g) H_{EB} of the Au(10 nm)/$Fe_{21}Ni_{79}$(0.7 nm)/as-grown (1 and 2 ML) and annealed 1-ML FeSe/STO films as a function of temperature.

of sample 1 measured at different temperatures. Shown in Fig. 4(i), T_B is ~140 K, meaning that $T_N \geq 140$ K for the 1-ML as-grown FeSe/STO film. More data on different samples of 1-ML films can be found in the SM [27]. The T_N value of the as-grown 1-ML FeSe/STO film is much higher than the reported highest T_N value (~55 K) of bulk FeSe under high pressure [9].

The MEBE depends on the competition between the interfacial energy J_{int} at the ferromagnet-antiferromagnet interface and the anisotropy energy $K_{\text{AFM}}t_{\text{AFM}}$ of the AFM layer, where K_{AFM} and t_{AFM} are the anisotropy constant and the thickness of the AFM layer, respectively. The condition $K_{\text{AFM}}t_{\text{AFM}} \geq J_{\text{int}}$ or $t_{\text{AFM}} \geq J_{\text{int}}/K_{\text{AFM}}$ is required for observation of the MEBE [28,40], meaning that a critical AFM thickness is needed for the MEBE [28,40]. In $Fe_{21}Ni_{79}$/FeSe/STO, J_{int} is relatively weak because the interfacial coupling occurs indirectly between the Fe/Ni atoms of $Fe_{21}Ni_{79}$ and the Fe atoms of FeSe through the Se atoms, which means that the critical AFM thickness in $Fe_{21}Ni_{79}$/FeSe/STO would be very thin. This is why we can observe the MEBE even in 1-ML-thick FeSe/STO films.

Furthermore, we carried out measurements on the as-grown 2-ML FeSe/STO films. The Au(10 nm)/$Fe_{21}Ni_{79}$(0.7 nm)/FeSe(2 ML)/STO sample exhibits the MEBE at low temperature after FC, indicating that 2-ML FeSe/STO film also has the AFM order. T_B is determined to be ~180 K [Fig. 4(i)], which is larger than that of 1-ML film, as expected due to the increased thickness of the AFM layer [26,28]. Interestingly, the T_B value of 2-ML FeSe/STO films is already similar to that of 100-ML FeSe/STO film, implying that the interlayer magnetic interaction is much weaker than the intralayer interaction, compatible with the layered structure of FeSe.

Finally, we try to get some insight into why AFM order exists in FeSe/STO films. Although the reason why bulk FeSe has no magnetic order is under debate [41–45], strong AFM fluctuations have been observed in neutron scattering experiments [46,47]. A DFT calculation has suggested that tensile stress could enhance the AFM interaction [18]. However, 100-ML FeSe/STO films already have a very similar lattice constant to bulk FeSe [12], but we still observed the MEBE. Therefore, we think that the strain effect plays a very minor or a negligible role for thick FeSe/STO films. In fact, although thick film and bulk crystal have the same lattice constant, they have very different microscopic properties. First, there are a number of Fe vacancies and domain walls of nematicity in FeSe/STO films [48]. Second, the strength of nematicity in FeSe/STO is much larger than that in bulk FeSe [48,49]. Third, a very recent STM study on FeSe/STO films observed a stripe-type charge ordering that does not exist in bulk FeSe, and the charge ordering is pinned in the vicinity of Fe vacancies, as well as domain walls of nematicity [48]. The pinned charge order is quantitatively comparable to a magnetic channel predicted theoretically [50]. In other words, impurities (or defects) could help to pin the magnetic fluctuations and could form a relatively long-range AFM order. The existence of AFM order could be the reason why superconductivity does not

recover in thick FeSe/STO films. On the other side, it is much more complicated in 1-ML films. Strong tensile stress and impurities (or defects) coexist [11,15,51]. Tensile stress enhances the interaction, while impurities or defects help to pin the AFM order, so we cannot rule out any of them for 1-ML films. Annealing process can inject electrons into the first ML. Interactions between local magnetic moments through mobile electrons would prefer the FM state where Hund coupling to dominate. Therefore, the competition between AFM and FM interactions could destroy the AFM order and eventually form superconductivity in 1-ML films. There could be other possibilities that could destroy the AFM order during the annealing process, and more theoretical input will be needed to fully understand the magnetic property of as-grown FeSe/STO films in the future.

In summary, we observed the AFM order in both 100-ML and 1-ML FeSe/STO films before electron doping by MEBE measurements. The low limit of the Néel temperature of 1-ML film is about 140 K. Our findings provide very important information for a comprehensive understanding of the novel properties of FeSe/STO films.

We acknowledge Chunlei Gao, Wei Ku, and Weijiong Chen for the discussions. This work was supported by the Ministry of Science and Technology of China (Grants No. 2016YFA0301003, No. 2016YFA0300403, and No. 2017YFA0303202) and the National Natural Science Foundation of China (Grants No. U1632272, No. 11574201, No. 11521404, No. 11674224, No. 11790313, No. 11727808, No. 11674159, and No. 51471086). D. Q. acknowledges support from the Changjiang Scholars Program. This research used resources of the Advanced Light Source, which is a DOE Office of Science User Facility under Contract No. DE-AC02-05CH11231.

Y. Z. and L. M. contributed equally to this work.

*dqian@sjtu.edu.cn
†dwu@nju.edu.cn

[1] P. C. Dai, J. P. Hu, and E. Dagotto, Nat. Phys. **8**, 709 (2012).
[2] P. A. Lee, N. Nagaosa, and X.-G. Wen, Rev. Mod. Phys. **78**, 17 (2006).
[3] H. Hosono and K. Kuroki, Physica (Amsterdam) **514C**, 399 (2015).
[4] J. Paglione and R. L. Greene, Nat. Phys. **6**, 645 (2010).
[5] D. J. A. Scalapino, Rev. Mod. Phys. **84**, 1383 (2012).
[6] F. Hsu *et al.*, Proc. Natl. Acad. Sci. U.S.A. **105**, 14262 (2008).
[7] S. Medvedev *et al.*, Nat. Mater. **8**, 630 (2009).
[8] M. Bendele, A. Amato, K. Conder, M. Elender, H. Keller, H.-H. Klauss, H. Luetkens, E. Pomjakushina, A. Raselli, and R. Khasanov, Phys. Rev. Lett. **104**, 087003 (2010).
[9] M. Bendele, A. Ichsanow, Yu. Pashkevich, L. Keller, Th. Strässle, A. Gusev, E. Pomjakushina, K. Conder, R. Khasanov, and H. Keller, Phys. Rev. B **85**, 064517 (2012).
[10] T. Terashima *et al.*, J. Phys. Soc. Jpn. **84**, 063701 (2015).
[11] Q. Y. Wang *et al.*, Chin. Phys. Lett. **29**, 037402 (2012).
[12] S. Tan *et al.*, Nat. Mater. **12**, 634 (2013).
[13] S. He *et al.*, Nat. Mater. **12**, 605 (2013).
[14] Z. Zhang, Y.-H. Wang, Q. Song, C. Liu, R. Peng, K. A. Moler, D. Feng, and Y. Wang, Science Bull. **60**, 1301 (2015).
[15] J. Ge, Z.-L. Liu, C. Liu, C.-L. Gao, D. Qian, Q.-K. Xue, Y. Liu, and J.-F. Jia, Nat. Mater. **14**, 285 (2015).
[16] B. Li, Z. W. Xing, G. Q. Huang, and D. Y. Xing, J. Appl. Phys. **115**, 193907 (2014).
[17] J. J. Lee *et al.*, Nature (London) **515**, 245 (2014).
[18] H.-Y. Cao, S. Tan, H. Xiang, D. L. Feng, and X.-G. Gong, Phys. Rev. B **89**, 014501 (2014).
[19] K. Liu, B.-J. Zhang, and Z.-Y. Lu, Phys. Rev. B **91**, 045107 (2015).
[20] K. Liu, Z.-Y. Lu, and T. Xiang, Phys. Rev. B **85**, 235123 (2012).
[21] H.-Y. Cao, S. Chen, H. Xiang, and X.-G. Gong, Phys. Rev. B **91**, 020504(R) (2015).
[22] Z. F. Wang *et al.*, Nat. Mater. **15**, 968 (2016).
[23] K. Nakayama, Y. Miyata, G. N. Phan, T. Sato, Y. Tanabe, T. Urata, K. Tanigaki, and T. Takahashi, Phys. Rev. Lett. **113**, 237001 (2014).
[24] T. Shimojima *et al.*, Phys. Rev. B **90**, 121111(R) (2014).
[25] M. D. Watson *et al.*, Phys. Rev. B **91**, 155106 (2015).
[26] J. Nogués and I. K. J. Schuller, J. Magn. Magn. Mater. **192**, 203 (1999).
[27] See Supplemental Material at http://link.aps.org/supplemental/10.1103/PhysRevLett.120.097001 for methods of data analysis, transport properties, FeTe films, ARPES and interfacial effects.
[28] A. E. Berkowitz and K. J. Takano, J. Magn. Magn. Mater. **200**, 552 (1999).
[29] D. Huang and J. E. Hoffman, Annu. Rev. Condens. Matter Phys. **8**, 311 (2017).
[30] W. Zhao *et al.*, arXiv:1701.03678.
[31] Y. C. Tian *et al.*, Phys. Rev. Lett. **116**, 107001 (2016).
[32] F. Li *et al.*, Phys. Rev. B **91**, 220503(R) (2015).
[33] M. A. Tomaz, D. C. Ingram, G. R. Harp, D. Lederman, E. Mayo, and W. L. O' Brien, Phys. Rev. B **56**, 5474 (1997).
[34] F. Wilhelm *et al.*, Phys. Rev. Lett. **85**, 413 (2000).
[35] F. Wilhelm, M. Angelakeris, N. Jaouen, P. Poulopoulos, E. Th. Papaioannou, Ch. Mueller, P. Fumagalli, A. Rogalev, and N. K. Flevaris, Phys. Rev. B **69**, 220404(R) (2004).
[36] C.-Y. Moon and H. J. Joon Choi, Phys. Rev. Lett. **104**, 057003 (2010).
[37] W. Bao *et al.*, Phys. Rev. Lett. **102**, 247001 (2009).
[38] M. Enayat *et al.*, Science **345**, 653 (2014).
[39] S. Demirdis, Physica (Amsterdam) **474B**, 53 (2015).
[40] A. P. Malozemoff, Phys. Rev. B **37**, 7673 (1988).
[41] F. Wang, A. K. Steven, and D.-H. Lee, Nat. Phys. **11**, 959 (2015).
[42] J. K. Glasbrenner, I. I. Mazin, H. O. Jeschke, P. J. Hirschfeld, R. M. Fernandes, and R. Valentí, Nat. Phys. **11**, 953 (2015).

[43] R. Yu and Q. Si, Phys. Rev. Lett. **115**, 116401 (2015).
[44] A. V. Chubukov, R. M. Fernandes, and J. Schmalian, Phys. Rev. B **91**, 201105(R) (2015).
[45] K. Liu, Z.-Y. Lu, and T. Xiang, Phys. Rev. B **93**, 205154 (2016).
[46] Q. Wang *et al.*, Nat. Commun. **7**, 12182 (2016).
[47] Q. Wang *et al.*, Nat. Mater. **15**, 159 (2016).
[48] W. Li *et al.*, Nat. Phys. **13**, 957 (2017).
[49] Y. Zhang *et al.*, Phys. Rev. B **94**, 115153 (2016).
[50] Y.-T. Tam, D.-X. Yao, and W. Ku, Phys. Rev. Lett. **115**, 117001 (2015).
[51] F. Li *et al.*, 2D Mater. **3**, 024002 (2016).